

## Structural superfluid–Mott-insulator transition for a Bose gas in multirods

Omar Abel Rodríguez-López<sup>1,\*</sup>, M. A. Solís,<sup>1,†</sup> and J. Boronat<sup>2,‡</sup>

<sup>1</sup>*Instituto de Física, Universidad Nacional Autónoma de México, Apartado Postal 20-364, 01000 Ciudad de México, Mexico*

<sup>2</sup>*Departament de Física, Universitat Politècnica de Catalunya, Campus Nord B4-B5, E-08034 Barcelona, Spain*



(Received 18 September 2020; revised 22 December 2020; accepted 22 December 2020; published 14 January 2021)

We report on a structural superfluid–Mott-insulator (SF-MI) quantum phase transition for an interacting one-dimensional Bose gas within permeable multirod lattices, where the rod lengths are varied from zero to the lattice period length. We use the *ab initio* diffusion Monte Carlo method to calculate the static structure factor, the insulation gap, and the Luttinger parameter, which we use to determine if the gas is a superfluid or a Mott insulator. For the Bose gas within a *square* Kronig-Penney (KP) potential, where barrier and well widths are equal, the SF-MI coexistence curve shows the same qualitative and quantitative behavior as that of a typical optical lattice with equal periodicity but slightly larger height. When we vary the width of the barriers from zero to the length of the potential period, keeping the height of the KP barriers, we observe a way to induce the SF-MI phase transition. Our results are of significant interest, given the recent progress on the realization of optical lattices with a subwavelength structure that would facilitate their experimental observation.

DOI: [10.1103/PhysRevA.103.013311](https://doi.org/10.1103/PhysRevA.103.013311)

### I. INTRODUCTION

Phase transitions are ubiquitous in condensed-matter physics. In particular, at very low temperatures, quantum phase transitions are the onset to distinguish new phenomena in quantum many-body systems. Following the realization of a Bose-Einstein condensate (BEC) in 1995 [1,2], a new and successful research line has been to study BECs within periodic optical lattices. It has been possible to study the properties and behavior of atomic gases trapped in three-dimensional (3D) multilayers, multitubes, or a simple cubic array of dots through the superposition of two opposing lasers in one, two, or three mutually perpendicular directions [3,4], respectively. One of the most exciting achievements has been the observation of the superfluid (SF) to Mott-insulator (MI) phase transition in a BEC with repulsive interactions, held both in 3D [3,5] and one-dimensional (1D) [6] optical lattices.

Although there have been great advances in the creation of many types of optical lattices, efforts are still being made to overcome their limited spatial resolution, which is of the order of one-half the laser wavelength  $\lambda_{OL}/2$ , to manipulate atoms. Recently, there has been a significant interest and advances in developing tools to surpass the diffraction limit, not only in the field of cold atoms but also in nanotechnology [7,8]. Nowadays, the physical realization of optical lattices formed by subwavelength (ultranarrow) optical barriers of width below  $\lambda_{OL}/50$  [9–12] is a reality. These so-called subwavelength optical lattices (SWOLs) can be seen as a very close experimental realization of a sequence of Dirac- $\delta$  functions, forming the well-known Dirac comb potential [13], and could be useful

to test many mean-field calculations on the weakly interacting Bose gas in this kind of potentials [14–18]. In the near future, we might see the realization of complex subwavelength optical lattices, including multiscale design, as a niche to observe new quantum phenomena [11,19]. From the point of view of theoretical simplicity, adaptable periodic structures ranging from the subwavelength to typical optical lattices could be simulated and engineered by applying an external Kronig-Penney (KP) potential, for example, to a quantum gas.

In this paper, we analyze the physical properties of a degenerate interacting 1D Bose gas in a lattice formed by a succession of permeable rods at zero temperature. To create this multirod lattice, we apply the KP potential [20]

$$V_{KP}(z) = V_0 \sum_{j=-\infty}^{\infty} \{\Theta[z - (jl + a)] - \Theta[z - (j + 1)l]\}, \quad (1)$$

to the gas, where  $V_0$  is the barrier height and  $\Theta(z)$  the Heaviside step function. The rods, distributed along the  $z$  direction, have width  $b$ , and are separated by empty regions of length  $a$ , such that the lattice period is  $l \equiv a + b$ . Here, we use the KP potential to study quantum gases due to its relatively simple shape, robustness, and versatility while preserving the system essence coming from the periodicity of its structure. We use it to model a typical optical lattice  $V(z) = V_0 \sin^2(k_{OL}z)$ , with  $k_{OL} = 2\pi/\lambda_{OL}$ , in the symmetric case  $b = a$ . Also, we model the subwavelength optical barriers in a SWOL through a Kronig-Penney lattice with  $b \ll a$ . Furthermore, we take advantage of the KP potential versatility by defining a parameter  $b/a$ , and analyze how its variation affects the ground-state properties of the Bose gas within a fixed-period multirod lattice. Then, we show a structural mechanism to induce a reentrant, commensurate SF-MI-SF quantum phase transition, by varying the ratio  $b/a$  while keeping the interaction strength and lattice period fixed. We propose that this transition,

\*Corresponding author: oarodriguez.mx@gmail.com

†masolis@fisica.unam.mx

‡jordi.boronat@upc.edu

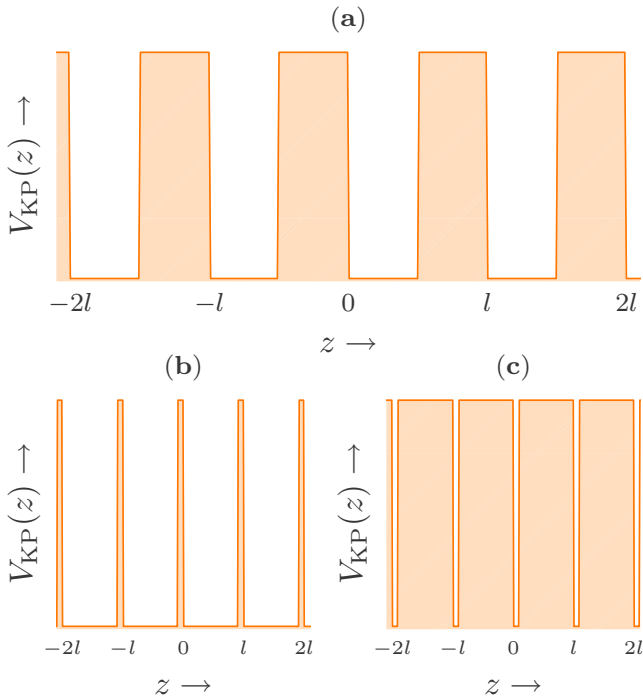


FIG. 1. Multirod lattices: (a) *square* lattice with  $b/a = 1$ ; (b) very thin lattice with  $b/a = 1/10$ ; (c) lattice with very broad barriers,  $b/a = 10$ .

infeasible in experiments with typical optical lattices under similar conditions, could be observed in experiments with cold atoms in SWOLs.

## II. MODEL AND THEORY

Our analysis relies on the *ab initio* diffusion Monte Carlo (DMC) method [21], adapted for the calculation of pure estimators through the forward-walking technique. The DMC method solves stochastically the many-body Schrödinger equation, providing exact results for the ground state of the system within some statistical noise. In Fig. 1, we show three faces of the KP potential depending on the ratio  $b/a$  while keeping  $V_0$  and  $l$  fixed: (a) the symmetric case where  $b = a$ , which is our reference potential; (b) when the barriers become very thin, i.e.,  $b \ll a$ ; and (c) when  $b \gg a$ . The limits  $b/a \rightarrow 0$  and  $b/a \rightarrow \infty$  convert the KP potential in constant potentials  $V_{\text{KP}} = 0$  and  $V_0$ , respectively. The bosonic particles interact through a contactlike, repulsive potential of arbitrary magnitude. Consequently, our system corresponds to the Lieb-Liniger (LL) Bose gas [22] within the multirod lattice Eq. (1). The Hamiltonian of the system with  $N$  bosons is

$$\hat{H} = -\frac{\hbar^2}{2m} \sum_{i=1}^N \left( \frac{\partial^2}{\partial z_i^2} + V_{\text{KP}}(z_i) \right) + g_{1\text{D}} \sum_{i<j}^N \delta(z_i - z_j), \quad (2)$$

where  $m$  is the mass of the particles,  $g_{1\text{D}} \equiv 2\hbar^2/ma_{1\text{D}}$  is the interaction strength, and  $a_{1\text{D}}$  is the one-dimensional scattering length. In the absence of the multirod lattice, we recover the LL Bose gas, which is exactly solvable for any magnitude of the dimensionless interaction parameter  $\gamma \equiv mg_{1\text{D}}/\hbar^2 n_1 = 2/n_1 a_{1\text{D}}$ , with  $n_1 = N/L$  the linear density.

The presence of a lattice can produce a quantum phase transition in the system from a superfluid state to a Mott-insulator state or vice versa, commonly known as *Mott transition* [5,6,23]. In deep optical lattices, that is, when the lattice height is way larger than the recoil energy  $E_R = \hbar^2 k_{\text{OL}}^2/2m$ , the well-known Bose-Hubbard (BH) model [3,5,6,24–26] captures the essence of the transition. According to this model, the competition between the on-site interaction  $U$  and the hopping energy  $J$  between adjacent lattice sites drives the transition from the SF to the MI state. In the Mott-insulator state, each lattice site contains the same number of particles. On the other hand, the SF-MI transition can be also studied using the low-energy description of the system given by the Luttinger liquid theory and the quantum sine-Gordon (SG) Hamiltonian [23,27–29]. In this approach, two system-dependent quantities, the speed of sound  $c_s$  and the Luttinger parameter  $K = \hbar\pi n_1/mc_s$ , play a central role in the description of the ground state. In particular, for any commensurate filling  $n_1 l = j/p$ , with  $j$  and  $p$  integers, the system can undergo a SF-MI transition when  $K$  takes the critical value  $K_c = 2/p^2$  [23,28], where  $p$  is the commensurability order. For  $p = 1$ , i.e., for an integer number of bosons per lattice site,  $K_c = 2$ . The 1D Bose gas remains superfluid while  $K > K_c$ , and variations in the interaction strength and the lattice height can push  $K$  towards  $K_c$ . The excitation energy spectrum is nongapped and increases linearly with the quasimomentum as  $E(k) = c_s \hbar |k|$  in the SF state [27,30], whereas it develops an excitation gap  $\Delta$  in the MI phase,  $E(k) = \sqrt{(c_s \hbar |k|)^2 + \Delta^2}$  [23]. Remarkably, in 1D gases, an arbitrarily weak periodic potential is enough to drive a Mott transition provided that the interactions are sufficiently strong [6,29].

A fingerprint of the Mott transition can be obtained from the static structure factor  $S(k)$  [31,32]:

$$S(k) \equiv \frac{1}{N} (\langle \hat{n}_{1,k} \hat{n}_{1,-k} \rangle - |\langle \hat{n}_{1,k} \rangle|^2), \quad (3)$$

where the operator  $\hat{n}_{1,k}$  is the Fourier transform of the density operator  $\hat{n}_1(z) \equiv \sum_{j=1}^N \delta(z - z_j)$ . For small momenta,  $S(k)$  is sensitive to the collective excitations of the system. For high- $k$  values,  $S(k)$  approximates to the model-independent value  $\lim_{k \rightarrow \infty} S(k) = 1$ . Furthermore, the low-momenta behavior of the energy spectrum  $E(k)$  is related to  $S(k)$  through the well-known Feynman relation [32–34],  $E(k) \equiv \hbar^2 k^2 / [2mS(k)]$ . This equation gives an upper bound to the excitation energies in terms of the static structure factor. Using this expression, we can estimate both the speed of sound  $c_s$  and the energy gap  $\Delta$  from the low-momenta behavior of  $S(k)$ . In the SF phase,  $\Delta = 0$ , and  $(c_s/v_F)^{-1} = 2k_F \lim_{k \rightarrow 0} S(k)/k$ , where  $k_F = \pi n_1$  is the Fermi momentum and  $v_F = \hbar k_F/m$  is the Fermi velocity. Also,  $K = (c_s/v_F)^{-1}$ . In contrast, in the MI phase,  $S(k)$  grows quadratically with  $k$  when  $k \rightarrow 0$ .

## III. TRANSITION IN A SYMMETRIC LATTICE

We study the SF-MI transition at unit-filling  $n_1 l = 1$  and  $b = a$ , i.e., our system has, on average, one boson per lattice site. We determine the Mott transition by calculating  $K$  as a function of the interaction strength  $\gamma$  and the lattice height  $V_0$ . The boundary between the SF and MI phases corresponds to the condition  $K(\gamma, V_0) = 2$ . In Fig. 2(a), we show the

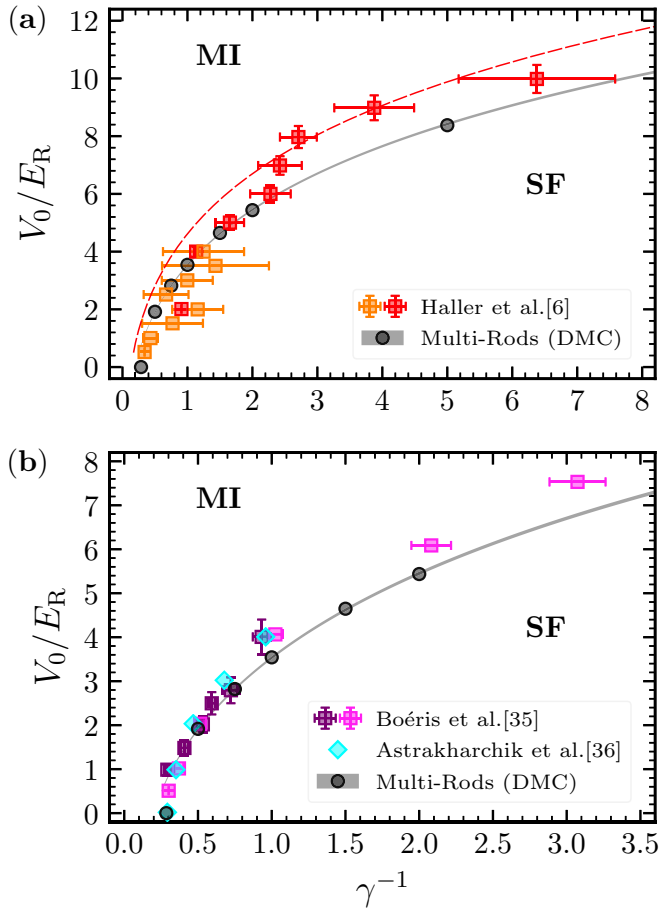


FIG. 2. Phase diagram of the 1D Bose gas in a square multirods potential at zero temperature. The region above the critical points is the Mott-insulator (MI) phase, while the region below corresponds to the superfluid (SF) phase. (a) We compare our results (black circles) against experimental data from Ref. [6] (orange and red squares); the dashed, red curve is the transition line for an optical lattice according to Eq. (4) with  $(U/J)_c = 3.85$ . The gray line is the transition for  $(U/J)_c = 2.571(12)$ . (b) Comparison with data from Ref. [35] (purple and pink squares), as well as with simulation data from Ref. [36] (blue diamonds). Note that (b) is an amplification of (a) in the strongly interacting region.

DMC zero-temperature phase diagram  $V_0/E_R$  vs  $\gamma^{-1}$  for a 1D Bose gas in a square multirod lattice (black circles). In the same figure, we also show experimental data [6] (orange and red squares) for a 1D Bose gas in an optical lattice at commensurability  $n_1 \sim 2/\lambda_{OL}$ , with  $\lambda_{OL}/2$  the spatial period of the optical potential. Note that the recoil energy is  $E_R = \hbar^2 \pi^2 / 2ml^2$  since we require that both optical and multirod lattices have the same periodicity, that is  $l = \lambda_{OL}/2$ .

We observe that our results are close to but below the experimental data in the deep lattices zone, where the BH model accurately describes the physics of the lattice. According to the 1D BH model, for an optical lattice the SF-MI transition occurs at the critical ratio  $(U/J)_c = 3.85$  [37]. Since  $U = (\sqrt{2\pi}/\pi^2) E_R \gamma (n_1 \lambda_{OL}/2) (V_0/E_R)^{1/4}$  and  $J = (4/\sqrt{\pi}) E_R (V_0/E_R)^{3/4} \exp[-2\sqrt{(V_0/E_R)}]$ , it is possible to define a relation between the lattice height  $V_0$  and the

interaction strength  $\gamma$  at the transition [29,38]:

$$\frac{4V_0}{E_R} = \ln^2 \left[ \frac{2\sqrt{2}\pi}{\gamma} \left( \frac{U}{J} \right)_c \sqrt{\frac{V_0}{E_R}} \right]. \quad (4)$$

In Fig. 2(a), we show Eq. (4) for the BH critical value  $(U/J)_c = 3.85$  (dashed, red line). The BH transition line agrees with the experimental data for lattices as high as  $V_0 \geq 7E_R$ , but fails for shallow lattices, a behavior discussed in Ref. [6]. Remarkably, most of our DMC simulation results follow the law Eq. (4), with a smaller energy ratio,  $(U/J)_c = 2.571(12)$  (dark-gray line), except close to the transition point  $\gamma_c^{-1} = 0.28$  for  $V_0 = 0$ , where we do not expect a good fit since the BH model Eq. (4) predicts  $\gamma^{-1} \rightarrow \infty$  when  $V_0 \rightarrow 0$ . The range of  $V_0$  values for which the BH model fits the multirods DMC results is, in fact, quite large, starting from lattice heights as low as  $\approx 2E_R$ . As we can see in Fig. 2(a), the square multirod lattice is more insulating than an optical lattice with the same strength. Looking at the Fourier series expansion of  $V_{KP}(z)$ , and considering only up to second order, we obtain that  $V_{KP}(z) \approx \tilde{V}_0 [1 - \cos(2\pi z/l)]/2 = \tilde{V}_0 \sin^2(k_{OL}z)$ , where  $\tilde{V}_0 = 4V_0/\pi$ . Hence, the multirod lattice is roughly equivalent to an optical lattice with a larger height  $\tilde{V}_0$ ; accordingly, the SF-MI transition in the former should occur at smaller  $V_0$  than the latter; our numerical results corroborate this observation.

In Fig. 2(b), we focus our analysis on shallow lattices only, where we do not include the data of Ref. [6] to avoid excessive piling of data. We compare our results with two additional relevant sources: first, experimental and numerical data reported in Ref. [35] (purple and pink squares), and second, DMC data reported in Ref. [36] (blue diamonds). Overall, there is a noticeable overlap between our DMC results and the data from Refs. [35,36], which is stronger as the lattices get shallower. The differences between the results for both lattices become smaller as  $\gamma_c^{-1} \rightarrow 0.28$  and  $V_0 \rightarrow 0$ , just as expected since for both multirod and optical lattices the system resembles more the Lieb-Liniger gas. Experimental data from [6,35] in Figs. 2(a) and 2(b) seem to agree better with the BH model predictions for multirods (gray line) than Eq. (4) for an optical lattice with  $(U/J)_c = 3.85$  (dashed, red line). On the other hand, Ref. [35] reports an estimation of  $(U/J)_c = 3.36$ , for which Eq. (4) agrees better with experimental data than the BH model for multirods. Given the above, it is clear that the experimental uncertainties in the data reported in Ref. [6] do not allow for a good estimation of  $(U/J)_c$  at the transition.

Complementary information on the MI phase can be obtained through the estimation of the energy gap  $\Delta$ . We calculate  $\Delta$  as a function of  $V_0$  for both the multirod and optical lattices, with  $\gamma = 11$ . This particular value of  $\gamma$  corresponds to the one for available experimental data [6]. Under these conditions, the system is a strongly interacting gas in the MI phase. We plot our results in Fig. 3, together with the experimental energy gap reported in Ref. [6]. We observe a good agreement between our simulation results (for both lattices) and the experimentally measured gap, better than similar results for an optical lattice shown in Ref. [36]. However, there is a clear qualitative discrepancy for  $V_0 > 0.8E_R$ , since the experimental results show something like a plateau, while our results grow monotonically. For shallow lattices, the SG model correctly describes the system's low-energy

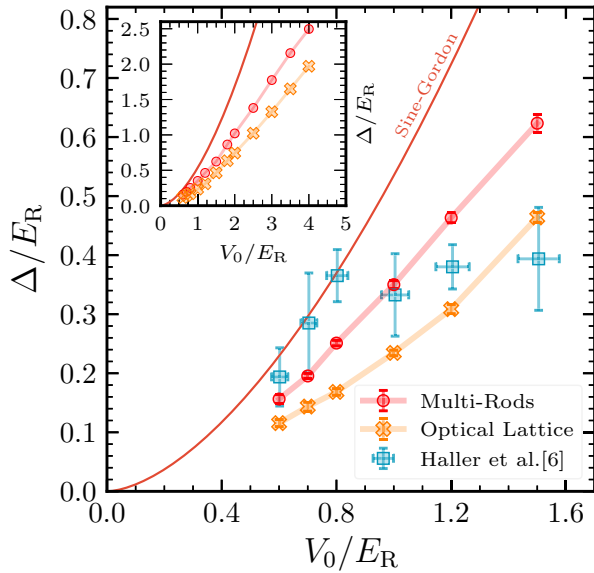


FIG. 3. Energy gap for the 1D Bose gas, with  $\gamma = 11$ , in a square multirod lattice (red circles) and in an optical lattice (orange crosses), calculated using DMC. Both lattices have the same height  $V_0$ . The blue squares show experimental gap data from Ref. [6]. The solid red line indicates the sine-Gordon model [6]. Inset: Gap behavior including lattices with  $V_0 \geq 1.6E_R$ .

properties; in particular, it predicts that  $\Delta$  increases with  $V_0$ , as our results. As commented in Ref. [36], the discussion on how good the modulation spectroscopy method for measuring  $\Delta$  is remains open. Finally, the gap as a function of  $V_0$ , for an optical lattice is smaller than the gap for a multirod lattice, so the latter is more insulating than the former, confirming the observation made after analyzing the results shown in Fig. 2.

#### IV. STRUCTURAL TRANSITION

Motivated by the recent studies on SWOLs, we extend the study of the interacting Bose gas within a square multirod lattice to a *nonsquare* multirod lattice, with special emphasis on describing the SF-MI quantum phase transition at commensurability  $n_1l = 1$ . We performed our analysis for a fixed interaction strength  $\gamma = 1$ . We calculate the speed of sound  $c_s$  from the low-momenta behavior of the static structure factor, and determine the  $V_0$  and  $b/a$  parameters such that  $K(b/a, V_0) = 2$ . In Fig. 4(a), we show the dependence of the parameter  $K = (c_s/v_F)^{-1}$  as a function of  $b/a$  in four lattices with heights  $V_0 = 3, 3.5, 4$ , and  $5$  times  $E_R$ . First, we can see that, depending on the value of the lattice ratio  $b/a$ ,  $K$  can be greater or smaller than  $K_c = 2$ . This result shows that the SF-MI transition can be triggered by changing the lattice's geometry if its height is large enough.

Variation of  $b/a$  always affects  $K$ ; however, although  $K$  could diminish (starting from a SF state), a phase transition may not necessarily occur for relatively shallow lattices. As one can see, for  $b/a \ll 1$  [thin barriers, see Fig. 1(b)] and  $b/a \gg 1$  [thin wells, see Fig. 1(c)], the gas becomes superfluid independently of  $V_0$ . On the one hand, as  $b/a$  diminishes and the barriers become thinner, the trapping effect of the lattice greatly reduces; in the limit  $b/a \rightarrow 0$  the system becomes

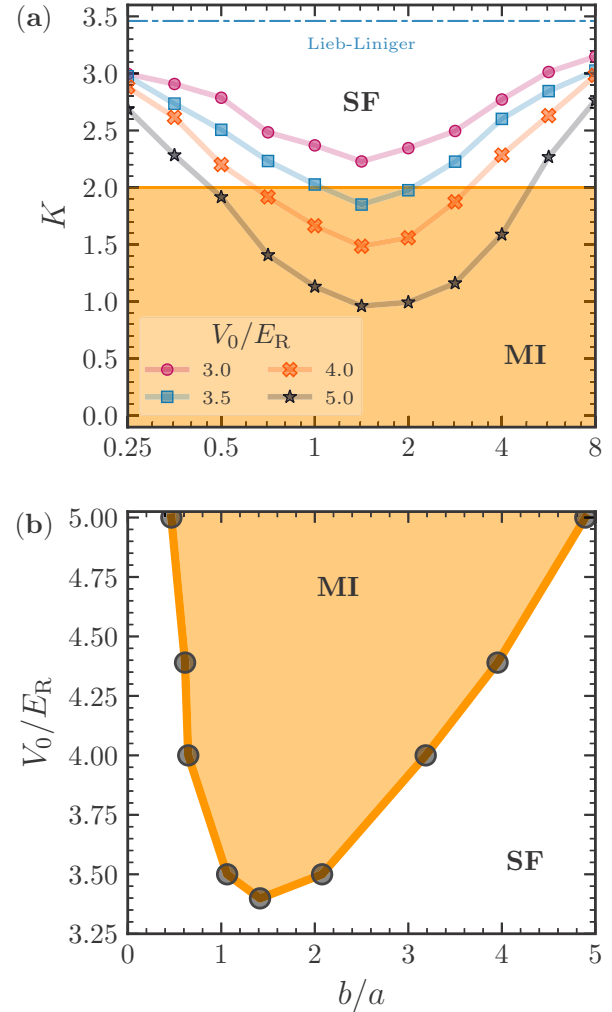


FIG. 4. (a)  $K$  parameter as a function of the lattice ratio  $b/a$ , for  $\gamma = 1$ . Independently of  $V_0$ , for both  $b/a \rightarrow 0$  and  $b/a \rightarrow \infty$ ,  $K$  approaches to the Lieb-Liniger Bose gas  $K = 3.43$  value. (b) SF-MI phase transition as a function of  $b/a$  and  $V_0/E_R$  for  $\gamma = 1$ . The statistical error of the results is smaller than the symbol size.

the LL gas. On the other hand, as  $b/a$  increases, the system tends to resemble more a succession of thin wells; in the limit  $b/a \rightarrow \infty$ , it becomes the LL gas subject to a constant potential of height  $V_0$ . Physically, there is no difference between both limits, except by a shift  $V_0$  in the total energy. Also, in both limits,  $K$  approaches the corresponding value for the LL model,  $K \approx 3.43$ . It is worth noticing that the minimum  $K$  in Fig. 4(a) occurs in the interval  $1 < b/a < 2$ , which interestingly shows that the largest trapping effect of the lattice does not correspond to the most symmetric case, i.e., the square lattice.

We show the zero-temperature phase transition diagram  $V_0/E_R$  vs  $b/a$  in Fig. 4(b). As noted before, the minimum interaction  $V_0$  to produce the Mott transition is slightly shifted to nonsquare potentials,  $b/a \simeq 1.4$ . When the asymmetry is  $b/a < 1$ , the strength  $V_0$  increases quite fast, favoring the stability of the SF phase. When  $b/a > 1.4$ ,  $V_0$  also increases but with a slightly smaller slope. The blob in the phase diagram is therefore not symmetric and interestingly shows the



possibility of a double transition SF-MI-SF for  $V_0 > 3.4$  by just changing the relation  $b/a$  keeping both  $V_0$  and  $\gamma$  constant. Note that Fig. 4(b) is a cross section of a MI tubular volume in the  $V_0/E_R$  vs  $\gamma^{-1}$  vs  $b/a$  diagram the asymmetric V-boat-hull shape surface of which contains the SF-MI phase coexistence line shown in Fig. 2(b).

## V. CONCLUSIONS

Using the *ab initio* DMC method we calculate the zero-temperature SF-MI quantum phase transition, in a  $V_0/E_R$  vs  $\gamma^{-1}$  diagram, for a 1D Bose gas with contact interactions within a square multirod lattice. We show and justify a notable similarity with the phase transition diagram of a Bose gas in a typical optical lattice by comparing it with several experimental and numerical data sources, finding that the multirod lattice favors the insulating phase. We also confirm that the BH model accurately predicts the transition in the regime of weak interactions and deep enough wells. For the Bose gas in both a multirod and optical lattices with the same strength and period, we calculate the energy gap  $\Delta$  as a function of the lattice height  $V_0$  for  $\gamma = 11$ . As expected, the gap is larger within the multirods lattice than in the optical lattice, validating what has already been observed in the phase transition diagrams. In the range of  $V_0$  values where experimental data exist for the gap, our results are of the same order of magnitude but do not match the experimental behavior that

shows something similar to a saturation with  $V_0$ . Finally, we show a structural mechanism to induce a robust reentrant, commensurate SF-MI-SF phase transition, triggered by the variation of the parameter  $b/a$  at fixed interaction strength and lattice period. We propose that such a mechanism could be experimentally implemented using the recently realized SWOLs, so the SF-MI structural phase transition could be observed.

## ACKNOWLEDGMENTS

We acknowledge partial support from the Programa de Apoyo a Proyectos de Investigación e Innovación Tecnológica (PAPIIT), the Dirección General de Asuntos del Personal Académico (DGAPA), and the Universidad Nacional Autónoma de México (UNAM) (PAPIIT-DGAPA-UNAM), under Grants No. IN-107616 and No. IN-110319. We also thank the Coordinación de Supercómputo de la Universidad Nacional Autónoma de México for the provided computing resources and technical assistance. This work has been partially supported by the Ministerio de Economía, Industria y Competitividad (MINECO, Spain) under Grant No. FIS2017-84114-C2-1-P. We acknowledge financial support from Secretaria d'Universitats i Recerca del Departament d'Empresa i Coneixement de la Generalitat de Catalunya, co-funded by the European Union Regional Development Fund (ERDF) within the ERDF Operational Program of Catalunya (QuantumCat Project No. 001-P-001644).

- 
- [1] M. H. Anderson, J. R. Ensher, M. R. Matthews, C. E. Wieman, and E. A. Cornell, *Science* **269**, 198 (1995).
  - [2] K. B. Davis, M. O. Mewes, M. R. Andrews, N. J. van Druten, D. S. Durfee, D. M. Kurn, and W. Ketterle, *Phys. Rev. Lett.* **75**, 3969 (1995).
  - [3] D. Jaksch, C. Bruder, J. I. Cirac, C. W. Gardiner, and P. Zoller, *Phys. Rev. Lett.* **81**, 3108 (1998).
  - [4] I. Bloch, *Nat. Phys.* **1**, 23 (2005).
  - [5] M. Greiner, O. Mandel, T. Esslinger, T. W. Hänsch, and I. Bloch, *Nature (London)* **415**, 39 (2002).
  - [6] E. Haller, R. Hart, M. J. Mark, J. G. Danzl, L. Reichsöllner, M. Gustavsson, M. Dalmonte, G. Pupillo, and H.-C. Nägerl, *Nature (London)* **466**, 597 (2010).
  - [7] X. Luo, *Adv. Mater.* **31**, 1804680 (2019).
  - [8] R. Halir, P. J. Bock, P. Cheben, A. Ortega-Moñux, C. Alonso-Ramos, J. H. Schmid, J. Lapointe, D.-X. Xu, J. G. Wangüemert-Pérez, Í. Molina-Fernández, and S. Janz, *Laser Photon. Rev.* **9**, 25 (2015).
  - [9] M. Łaącki, M. A. Baranov, H. Pichler, and P. Zoller, *Phys. Rev. Lett.* **117**, 233001 (2016).
  - [10] Y. Wang, S. Subhankar, P. Bienias, M. Łaącki, T.-C. Tsui, M. A. Baranov, A. V. Gorshkov, P. Zoller, J. V. Porto, and S. L. Rolston, *Phys. Rev. Lett.* **120**, 083601 (2018).
  - [11] S. Subhankar, P. Bienias, P. Titum, T.-C. Tsui, Y. Wang, A. V. Gorshkov, S. L. Rolston, and J. V. Porto, *New J. Phys.* **21**, 113058 (2019).
  - [12] T.-C. Tsui, Y. Wang, S. Subhankar, J. V. Porto, and S. L. Rolston, *Phys. Rev. A* **101**, 041603(R) (2020).
  - [13] E. Merzbacher, *Quantum Mechanics*, 2nd ed. (Wiley, New York, 1969).
  - [14] S. Theodorakis and E. Leontidis, *J. Phys. A: Math. Gen.* **30**, 4835 (1997).
  - [15] W. D. Li and A. Smerzi, *Phys. Rev. E* **70**, 016605 (2004).
  - [16] B. T. Seaman, L. D. Carr, and M. J. Holland, *Phys. Rev. A* **71**, 033609 (2005).
  - [17] X. Dong and B. Wu, *Laser Phys.* **17**, 190 (2007).
  - [18] O. A. Rodríguez-López and M. A. Solís, *J. Low Temp. Phys.* **198**, 190 (2020).
  - [19] A. K. Fedorov, V. I. Yudson, and G. V. Shlyapnikov, *Phys. Rev. A* **95**, 043615 (2017).
  - [20] R. de L. Kronig and W. G. Penney, *Proc. R. Soc. Lond. A* **130**, 499 (1931).
  - [21] J. Boronat and J. Casulleras, *Phys. Rev. B* **49**, 8920 (1994).
  - [22] E. H. Lieb and W. Liniger, *Phys. Rev.* **130**, 1605 (1963).
  - [23] T. Giamarchi, *Quantum Physics in One Dimension* (Oxford University, New York, 2003).
  - [24] M. P. A. Fisher, P. B. Weichman, G. Grinstein, and D. S. Fisher, *Phys. Rev. B* **40**, 546 (1989).
  - [25] T. D. Kühner and H. Monien, *Phys. Rev. B* **58**, R14741 (1998).
  - [26] L. Tarruell and L. Sanchez-Palencia, *Comptes Rendus Phys.* **19**, 365 (2018).
  - [27] F. D. M. Haldane, *Phys. Rev. Lett.* **47**, 1840 (1981).
  - [28] M. A. Cazalilla, R. Citro, T. Giamarchi, E. Orignac, and M. Rigol, *Rev. Mod. Phys.* **83**, 1405 (2011).
  - [29] H. P. Büchler, G. Blatter, and W. Zwerger, *Phys. Rev. Lett.* **90**, 130401 (2003).

- [30] F. D. Haldane, *J. Phys. C* **14**, 2585 (1981).
- [31] V. I. Yukalov, *J. Phys. Stud.* **11**, 55 (2007).
- [32] L. Pitaevskii and S. Stringari, *Bose-Einstein Condensation and Superfluidity*, 2nd ed. (Oxford University, New York, 2016).
- [33] R. P. Feynman, *Phys. Rev.* **94**, 262 (1954).
- [34] J. Steinhauer, R. Ozeri, N. Katz, and N. Davidson, *Phys. Rev. Lett.* **88**, 120407 (2002).
- [35] G. Boéris, L. Gori, M. D. Hoogerland, A. Kumar, E. Lucioni, L. Tanzi, M. Inguscio, T. Giamarchi, C. D’Errico, G. Carleo, G. Modugno, and L. Sanchez-Palencia, *Phys. Rev. A* **93**, 011601(R) (2016).
- [36] G. E. Astrakharchik, K. V. Krutitsky, M. Lewenstein, and F. Mazzanti, *Phys. Rev. A* **93**, 021605(R) (2016).
- [37] S. Rapsch, U. Schollwöck, and W. Zwerger, *Europhys. Lett.* **46**, 559 (1999).
- [38] I. Bloch, J. Dalibard, and W. Zwerger, *Rev. Mod. Phys.* **80**, 885 (2008).